NICST Internal Memo

Date: December 16, 2008
From: J. McIntire, T. Schwarting, and C. Pan
To: Bruce Guenther, Jim Butler, and Jack Xiong
Subject: SMWIR and LWIR Crosstalk Analysis Using VIIRS EDU FP-16 Part 2

References:

[1] NICST_MEMO_07_001, "VIIRS EDU VNIR Xtalk/Scatter Analysis using FP-16 part 1 OOB RSR Measurement Data," D. Moyer, N. Che, and J. Xiong, January 2, 2007.
[2] NICST_REPORT_06_019, "VIIRS EDU Xtalk/Scatter Analysis (FP-16 Part 1)," November 15, 2006.
[3] NICST_REPORT_06_023, "VIIRS EDU Xtalk/Scatter Analysis (FP-16 Part 2)," December 13, 2006.
[4] NICST_MEMO_08_031, "Shutter Map Investigation for VIIRS EDU FP-15 and FP-16," J. McInitre, T. Schwarting, and C. Pan, September 10, 2008.

1. Introduction

The VIIRS EDU FP-16 test measured the Out Of Band (OOB) crosstalk using the Spectral Measurement Assembly (SpMA). The primary purpose of this test was to evaluate the Relative Spectral Response (RSR). However, it is also possible to use this test in a crosstalk analysis of the OOB crosstalk to different slit positions [1-3]. This work focuses on the crosstalk analysis (as an expansion on previous work [3]) for the SMWIR and LWIR bands.

The FP-16 Part 2 test consists of three types of measurement: In Band (IB) with a Neutral Density (ND) filter, OOB without a ND filter, and band to point crosstalk at the center wavelength of each band (with a ND filter). The ND filter was used to provide a reduced illumination level. The first two measurements are the subject of this work.

A vertical slit is positioned spatially over the odd detectors in the sender band. Then the SpMA illuminates the sensor at wavelengths ranging from 1000 – 7100 nm (2000 – 16000 nm) for the SMWIR (LWIR) OOB UAIDs. The IB UAIDs cover only in band wavelengths (between the specified 1% limits). As FP-16 is a staring test, the background subtraction is generated using a shutter on the SpMA. Each collect contains eight scans which obey a cycle of two scans open followed by two scans closed. The data was collected in diagnostic mode and fixed high gain. The UAIDs, sender bands, type of measurement (IB or OOB), and wavelength range used here are listed in Table 1.

2. Data Processing

First, the DN is averaged over samples using three sigma rejection. Next, the shutter map is constructed via the method described in [4] with some minor modifications. Once the shutter order is determined, the shutter closed DN is subtracted from the shutter open DN, or

$$dn(\lambda,B,D,S) = \left\langle DN_{open}(\lambda,B,H,D,S) - DN_{closed}(\lambda,B,H,D,S) \right\rangle_H \quad (1)$$

where B, H, D, S, and λ represent band, HAM side, detector, subsample, and SpMA wavelength (or equivalently collect), respectively. As this is staring test, the dn is then averaged over HAM side. The dn is converted to radiance (L) via the equation

$$L(\lambda,B,D,S) = dn(\lambda,B,D,S) / g(B,D,S) \quad (2)$$

where g is the radiometric gain, determined from RC-05 for the LWIR and MWIR bands and RC-02 for the SWIR bands (both nominal plateau).

The OOB UAIDs saturate for some in band wavelengths, while the IB UAIDs do not saturate as a result of the ND filter. The transmittance of the ND filter is determined via the equation

$$\tau(B,D,S) = \left\langle \frac{dn_{ND}(\lambda,B,D,S)}{dn_{OOB}(\lambda,B,D,S)} \right\rangle_\lambda \quad (3)$$

where the average is over collects (or wavelengths). The only collects used to determine the transmittance are those for which the IB and OOB wavelengths overlap but have neither saturated nor have negligible dn. As an example, Figure 1 highlights (green) the region of overlap used in the transmittance calculation for band M8 (note that the IB UAID is plotted in red and OOB UAID is plotted in black). The calculated transmittance coefficients for the odd detectors in each band are listed in Table 2; in addition, the average of the odd detectors for each band (minus detectors that reach less than half the maximum measured dn for a particular band) is given at the bottom of Table 2. Those detectors used in the average are highlighted in green. The average transmittance value is used in the subsequent analysis. Note that the transmittance was not calculated for the even detectors as no measurements were conducted.

Once the transmittance is determined, the approximate SpMA radiance at a particular wavelength is evaluated using the following equation,

$$L_{spma}(\lambda,B_{ref},D,S) = \frac{dn_{MAX}(B_{ref},D,S)}{\tau(B_{ref})} \frac{R_{spma}(\lambda_{ref})}{R_{spma}(\lambda)} \quad (4)$$

where λ_{ref} is the center wavelength for a particular band and B_{ref} refers to the position of the slit. Here dn_{MAX} is the measured maximum response for the IB UAIDs. R_{spma} is the relative SpMA radiance. The SpMA radiance was measured by a pyrometer using a number of different gratings; however, no single grating covered the entire wavelength range for the SMWIR bands. These measurements were spliced together and the resulting SpMA RSR curve is shown in Figure 2.

The percent crosstalk is then constructed using this SpMA radiance, or

$$\%Crosstalk(\lambda,B,D,S) = 100 \frac{L(\lambda,B,D,S)}{L_{spma}(\lambda,B,D,S)} \quad (5)$$

This is the ratio of the radiance received to the approximate source radiance expressed in percent and is used to analyze the crosstalk / scatter in the OOB response.

3. Analysis

3.1 SMWIR

Figures 3 – 10 show the response as a function of wavelength for each SMWIR band. For each figure, the response for two detectors (upper and lower plots) is evaluated for a particular band at the slit positions listed in the legend. The middle detector graphs are consistent with the results reported in [3]. The center wavelengths for each band are marked at the bottom of every graph.

In Figure 3, the I3 subsample 1 (SS1) response is graphed for detectors 16 and 17. There is a large response (about 25 dn) in the both the M13 bandpass when the slit is over M13 and in the M8 bandpass when the slit is over M8 for the even detectors. The odd detectors show a large response (about 20 dn) for both slit positions M11 and M12 in their respective bandpasses as well as about 5 dn in the M13 bandpass when the slit is over M13. This pattern is reversed for subsample 2 (SS2). The negative response in the I3 bandpass when the slit is over I3 is the possible result of a readout error when band I3 is saturated. In addition, the spike at about 2400 nm at the M12 slit position is the possible result of a shutter map error.

Figure 4 graphs the response of I4 SS1 for the middle detectors 16 and 17. The even detectors show a response for the slit positions M10 and I3 (about 5 – 10 dn), M11 (roughly 30 dn), and M13 (about 10 dn) in their respective bandpasses. The odd detectors exhibit the same features with about 10 dn for I3, 25 dn for M10, 5 dn for M11, and 35 dn for M13 as well as 35 dn in the bandpass of M8 when the slit is positioned over M8. This pattern is reversed for subsample 2 (SS2).

The response of M8 for detectors 4 and 9 is plotted in Figure 5. Detector 9 shows the typical response for an odd detector in M8; about negative 5 dn in the M13 bandpass when the slit is over M13 and some small response when the slit is over M8 between 1400 – 2100 nm with a spike around 2100 of over 60 dn. Detector 4 shows some Out Of Family (OOF) behavior: there is a negative response in band for M8 when the slit is over M8; there is a 10 dn response in the bandpass of M10 (I3) when the slit is over M10 (I3); and the negative response in M13 is not present. Detector 6 also exhibits some OOF behavior.

The M9 response for detectors 4 and 9 is plotted in Figure 6. Detector 9 shows the typical response for an odd detector in M9; about negative 5 dn in the M13 bandpass when the slit is over M13, some small response when the slit is over M8 between 1400 – 2100 nm, and a negative response in band for M9 (possible readout error when M9 is saturated). Detector 4 behaves somewhat OOF as seen by a more pronounced possible readout error in band for M9 and 5 dn in the M11 bandpass when the slit is over M11. Detector 6 behaves similarly.

Figure 7 plots the response in M10 for detectors 4 and 9. Again, detector 9 provides an example of the typical response for an odd detector in M10; about negative 5 dn in the M13 bandpass when the slit is over M13 and some small response when the slit is over M8 between 1800 – 2300 nm. OOF behavior is observed in detector 4; the response in the M13 bandpass is now negligible and a negative response is observed on both sides of the in band M10 peak (within the 1% limits). A small response of about 5 dn is also observed in the M8 bandpass when the slit is over M8.

The M11 response for detectors 9 and 12 is plotted in Figure 8. Detector 9 shows the typical response for an odd detector in M11; about negative 5 dn in the M13 bandpass when the slit is over M13 and some small response when the slit is over M11 between 1700 – 1800 nm. Detector 12 exhibits OOF behavior; a 15 dn response is observed in the M12 bandpass when the slit is over M12, some small negative response (10 dn) is seen in the M9 bandpass when the slit is over M9, about negative 5 dn in the M13 bandpass when the slit is over M13, and a negative response is observed on both sides of the in band M11 peak (within the 1% limits).

Figure 9 plots the response in M12 for detectors 9 and 12. Again, detector 9 provides an example of the typical response for an odd detector in M12; about negative 5 dn in the M13 bandpass when the slit is over M13. OOF behavior is observed in detector 12; the same response in the M13 bandpass is observed and a negative response is observed on both sides of the in band M12 peak (within the 1% limits).

The M13 (high gain) response for detectors 4 and 9 is plotted in Figure 10. Detector 9 shows the typical response for an odd detector in M11. Detector 4 exhibits OOF behavior; a negative response is observed on both sides of the in band M13 peak (within the 1% limits) as well as a small response (5 – 10 dn) in the bandpasses of M8, M10, and I3 when the slit is positioned over M8, M10, and I3, respectively.

Figures 11 – 18 show the percent crosstalk as a function of wavelength for each SMWIR band. For each figure, the percent crosstalk is evaluated for a particular band at the slit positions listed in the legend. The center wavelengths for each band are marked at the bottom of every graph. Only the odd detectors were analyzed as the even detector did not receive direct illumination. In addition, the edge detectors were not fully illuminated due to source limitations and as a result are not analyzed here.

In Figure 11, the percent crosstalk observed in I3 SS1, detector 21 is shown. The upper plot shows the main peaks in the MWIR: there is a percent crosstalk of 30% in M12, 3 – 4% in M13, and about 1% in M11. The lower graph focuses on the same data at a smaller scale; percent crosstalk of between 0.5% and -1% is observed in the bandpass of I4 when the slit is over I4. In addition, I3 exhibits a percent crosstalk of between -0.1% and 0.1% over the entire wavelength range when the slit is over any MWIR band. Detector 23 shows some additional percent crosstalk in the M12 bandpass (40%) when the slit is over M12 as well as between -0.2% and 0.2% over the entire wavelength range when the slit is over any MWIR band. In contrast, the SWIR bands show much smaller fluctuations.

The percent crosstalk exhibited by I4 SS1, detector 17 is shown in Figure 12. The percent crosstalk from M10 and M11 are on the order of 0.1% while the M13 percent crosstalk is about 5%. Additionally, the percent crosstalk for slit positions over any of the MWIR fluctuates between 0.1% and -0.1% over the entire wavelength range. In contrast, the SWIR bands show much smaller fluctuations.

In Figure 13, the percent crosstalk observed in M8, detector 5 is shown. The main features in the percent crosstalk for M8 are the electronic crosstalk of -0.2% from the M13 bandpass when M13 is illuminated and the crosstalk of 0.2% from the I4 bandpass when I4 is illuminated. There is also a small amount of crosstalk at the M12 slit position between 3500 – 4100 nm (less than 0.05%).

The percent crosstalk observed in M9, detector 9 is plotted in Figure 14. The major feature is the electronic crosstalk of -0.15% from the M13 bandpass when M13 is illuminated. There is also a small amount of crosstalk at the M12 slit position between 3500 – 4100 nm (less than 0.05%) and at the I4 slit position between 3500 – 4000 nm (less than 0.1%).

In Figure 15, the percent crosstalk observed in M10, detector 5 is shown. The main features are the electronic crosstalk of -0.4% from the M13 bandpass when M13 is illuminated, the crosstalk of 0.3% from the I4 bandpass when I4 is illuminated, and also some crosstalk at the M12 slit position between 3500 – 4100 nm (less than 0.2%).

The M11, detector 9 percent crosstalk is plotted in Figure 16. Electronic crosstalk of -0.3% from the M13 bandpass is observed when M13 is illuminated as well as crosstalk of 0.2% from the I4 bandpass when I4 is illuminated and also some crosstalk at the M12 slit position between 3500 – 4100 nm (less than 0.1%).

For M12, detector 9, the percent crosstalk is shown in Figure 17. The only significant feature is the electronic crosstalk of -0.25% from the M13 bandpass is observed when M13 is illuminated.

In Figure 18, percent crosstalk for band M13 is plotted.

3.2 LWIR

Figures 19 – 23 show the response as a function of wavelength for each LWIR band. For each plot, the response is evaluated for a particular band at the slit positions listed in the legend. The center wavelengths for each LWIR band are marked at the bottom of every graph. As only one IB UAID was recorded for the LWIR, no percent crosstalk analysis was performed.

A small response of -10 dn in the M14 bandpass is observed in the I5 SS1, detector 27 response when the slit is over M14 (see Figure 19). No other detector in I5 behaves in this manner. Figure 20 shows almost no OOB response for sender band M14, detector 9.

However, detector 10 in M14 (also Figure 20) shows ±5 dn over the entire wavelength range for multiple slit positions; this detector is known to be noisy. Figure 21 shows some OOB response (about 5 – 10 dn) in M15, detector 9 when the slit is positioned over M15 at wavelengths between 7500 – 8500 nm. Similarly, OOB response (about 5 – 20 dn) is observed in both M16A, detector 9 (slit position M16A) and M16B, detector 9 (slit position M16B) between 7750 – 9250 nm in Figures 22 and 23, respectively. Figure 23 also shows the response for M16B detector 16. A small response of -10 dn in the M14 bandpass is observed in the M16B, detector 16 response when the slit is over M14. No other detector in M16B behaves in this manner.

4. Summary

- Negative crosstalk is evident from M13 into all other M bands (between -0.2% and -0.4%).
- Positive crosstalk is evident from M13 into both I bands (3 – 4% for I3 and 5% for I4).
- Positive crosstalk from M12 into I3 (30%), both positive and negative crosstalk from I4 into I3 (1%), and positive crosstalk from M11 into I3 (1%) are observed.
- Positive crosstalk from M12 into M8, M9, M10, and M11 (between 0.1% and 0.4%).
- Negative response IB probable result of readout error during saturation observed in I3 and M9.
- OOF detectors observed: detector 4 in bands M8, M9, M10, and M13; detector 6 in M8 and M9; and detector 12 in M11 and M12.
- OOB percent crosstalk into I3 and I4 from MWIR slit positions (±0.1 – 0.2%) over wavelength range 1000 – 7000 nm.
- Small OOB crosstalk observed in M15 (slit position M15) between 7500 – 8500 nm; small OOB crosstalk observed in M16A (slit position M16A) and M16B (slit position M16B) between 7750 – 9250 nm.

Acknowledgement

The sensor test data used in this document was provided by the SBRS testing team. Approaches for data acquisition and data reductions, as well as data extraction tools were also provided by the SBRS. We would like to thank the SBRS team for their support. The data analysis tools were developed by the NICST team, and we would like to extend our gratitude for their valued assistance.

Table 1: EDU FP-16 Part 2 UAIDs with corresponding sender bands.

UAID	Sender Band	IB / OOB	Wavelength range (nm)
2002548	M13	IB	3782 - 4340
2002549	M13	OOB	1000 - 7096
2002552	M12	IB	3401 - 4049
2002553	M12	OOB	1000 - 7187
2002558	I4	IB	3326 - 4166
2002559	I4	OOB	1000 - 7134
2002562	I3	IB	1506 - 1722
2002563	I3	OOB	990 - 7066
2002566	M10	IB	1506 - 1722
2002567	M10	OOB	1002 - 7096
2002570	M11	IB	2164 - 2344
2002571	M11	OOB	994 - 7201
2002574	M8	IB	1204 - 1276
2002575	M8	OOB	996 - 7208
2002584	M9	IB	1350 - 1409
2002585	M9	OOB	990 - 7199
2002588	M14	IB	8035 - 9115
2002589	M14	OOB	1800 - 16015
2002592	M15	OOB	1800 - 16167
2002596	M16A	OOB	1800 - 16097
2002600	M16B	OOB	2280 - 16097
2002603	I5	OOB	1804 - 16122

Table 2: Odd detector ND transmittance for all SMWIR bands and M14.

Detector	M13	M12	I4	I3	M10	M11	M8	M9	M14
1	0.0900	0.0722	0.0967	0.1079	0.0296	0.3736	0.0251	0.0070	0.3725
3	0.1038	0.0465	0.0688	0.0407	0.0149	0.0564	0.0133	0.0048	0.4482
5	0.1077	0.0495	0.0789	0.0229	0.0150	0.0545	0.0159	0.0048	0.3131
7	0.1077	0.0511	0.0886	0.0185	0.0152	0.0565	0.0169	0.0049	0.5741
9	0.1057	0.0513	0.0921	0.0172	0.0155	0.0562	0.0159	0.0049	0.3116
11	0.1055	0.0502	0.0934	0.0172	0.0156	0.0567	0.0156	0.0049	0.5530
13	0.1045	0.0507	0.0948	0.0177	0.0155	0.0562	0.0145	0.0048	0.5455
15	0.1020	0.0476	0.0935	0.0173	0.0153	0.0550	0.0146	0.0048	0.3048
17	~	~	0.0958	0.0172	~	~	~	~	~
19	~	~	0.0948	0.0174	~	~	~	~	~
21	~	~	0.0965	0.0177	~	~	~	~	~
23	~	~	0.0960	0.0176	~	~	~	~	~
25	~	~	0.0951	0.0172	~	~	~	~	~
27	~	~	0.0954	0.0173	~	~	~	~	~
29	~	~	0.0926	0.0176	~	~	~	~	~
31	~	~	0.0959	0.0173	~	~	~	~	~
Average	0.1053	0.0496	0.0941	0.0175	0.0154	0.0559	0.0156	0.0049	0.3098

Figure 1: IB (red) and OOB (black) response for M8. The data used to calculate the transmittance is highlighted in green.

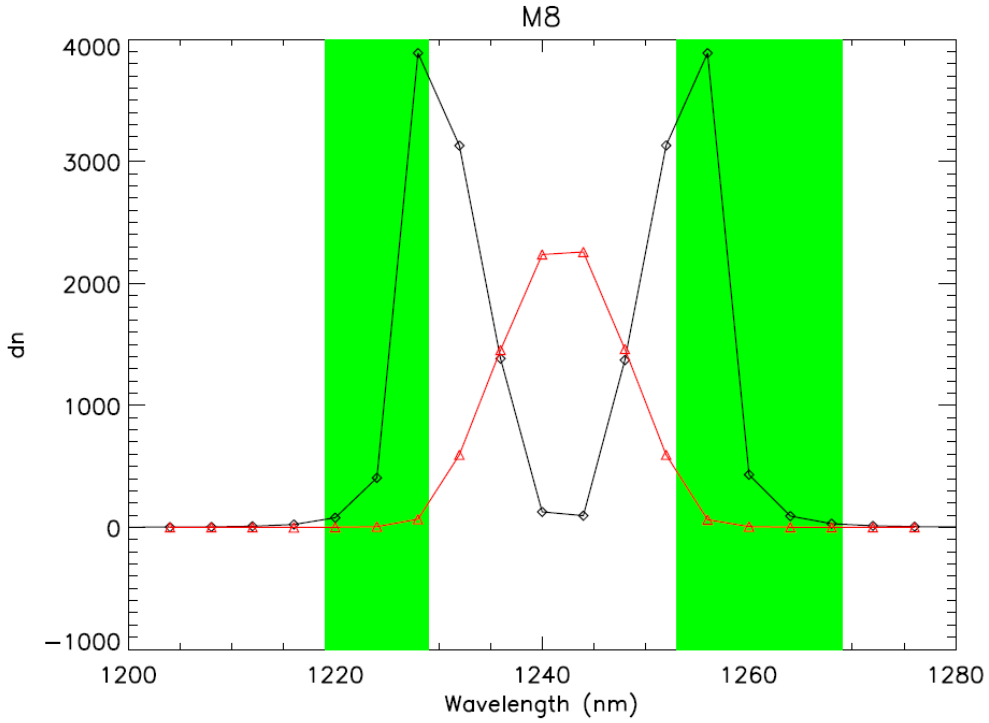

Figure 2: R_{spma} as a function of wavelength

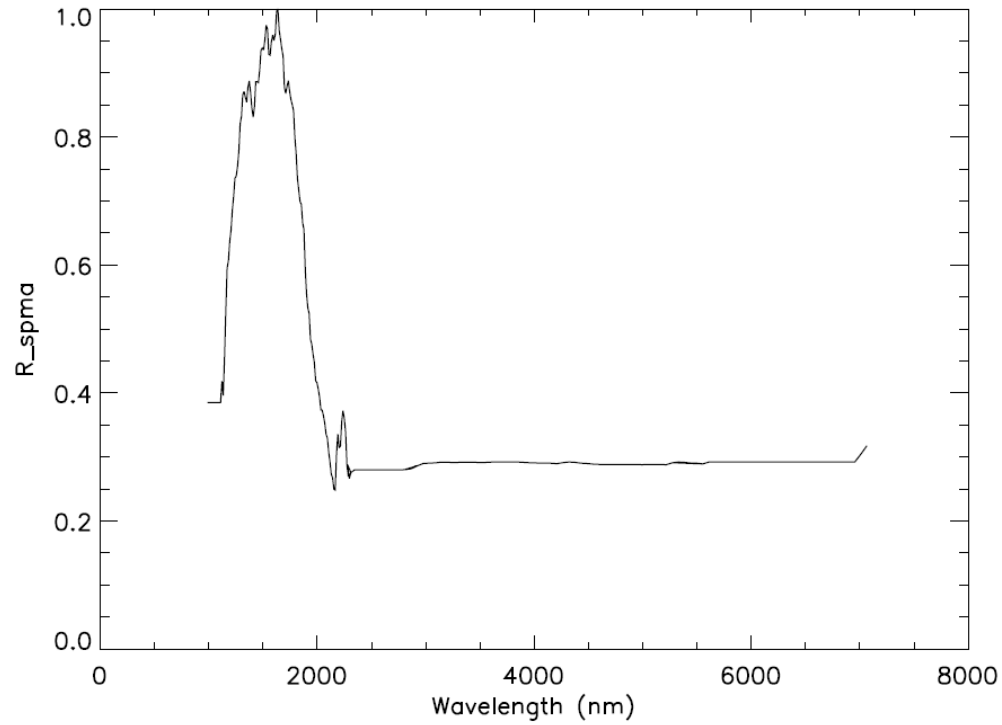

Figure 3: Response as a function of wavelength and slit position for the I3 SS1 detectors 16 and 17.

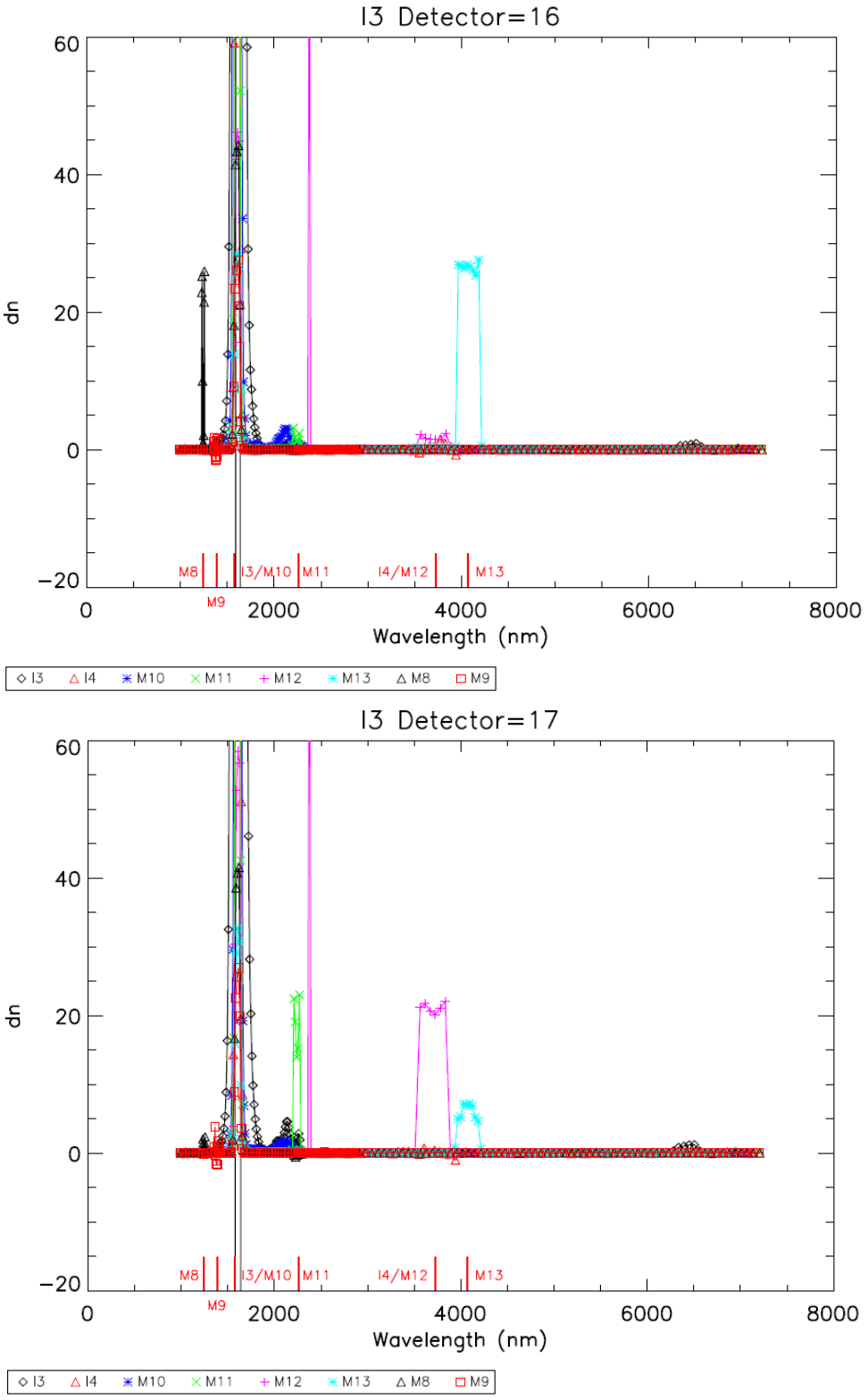

Figure 4: Response as a function of wavelength and slit position for the I4 SS1 detectors 16 and 17.

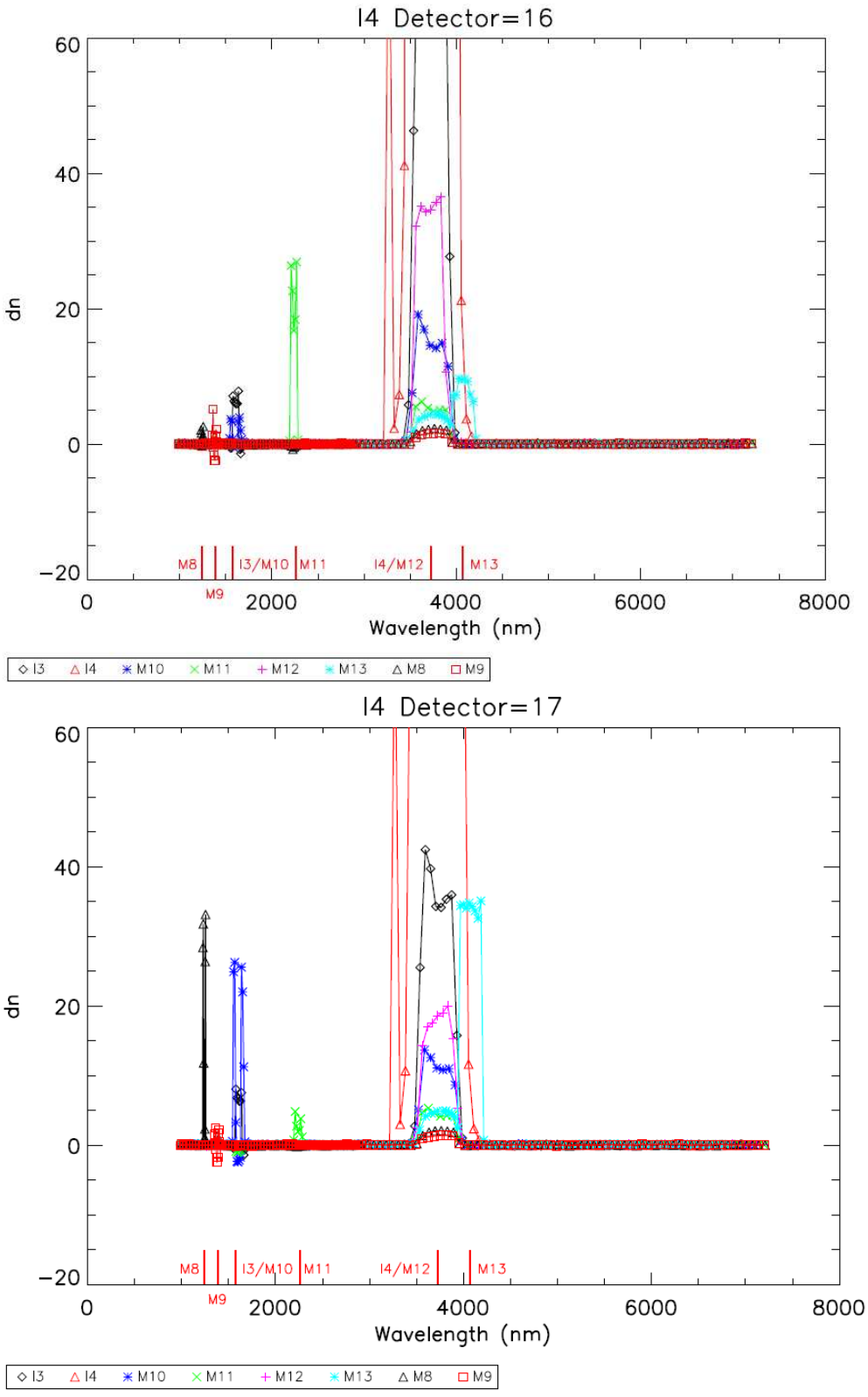

Figure 5: Response as a function of wavelength and slit position for the M8 detectors 4 and 9.

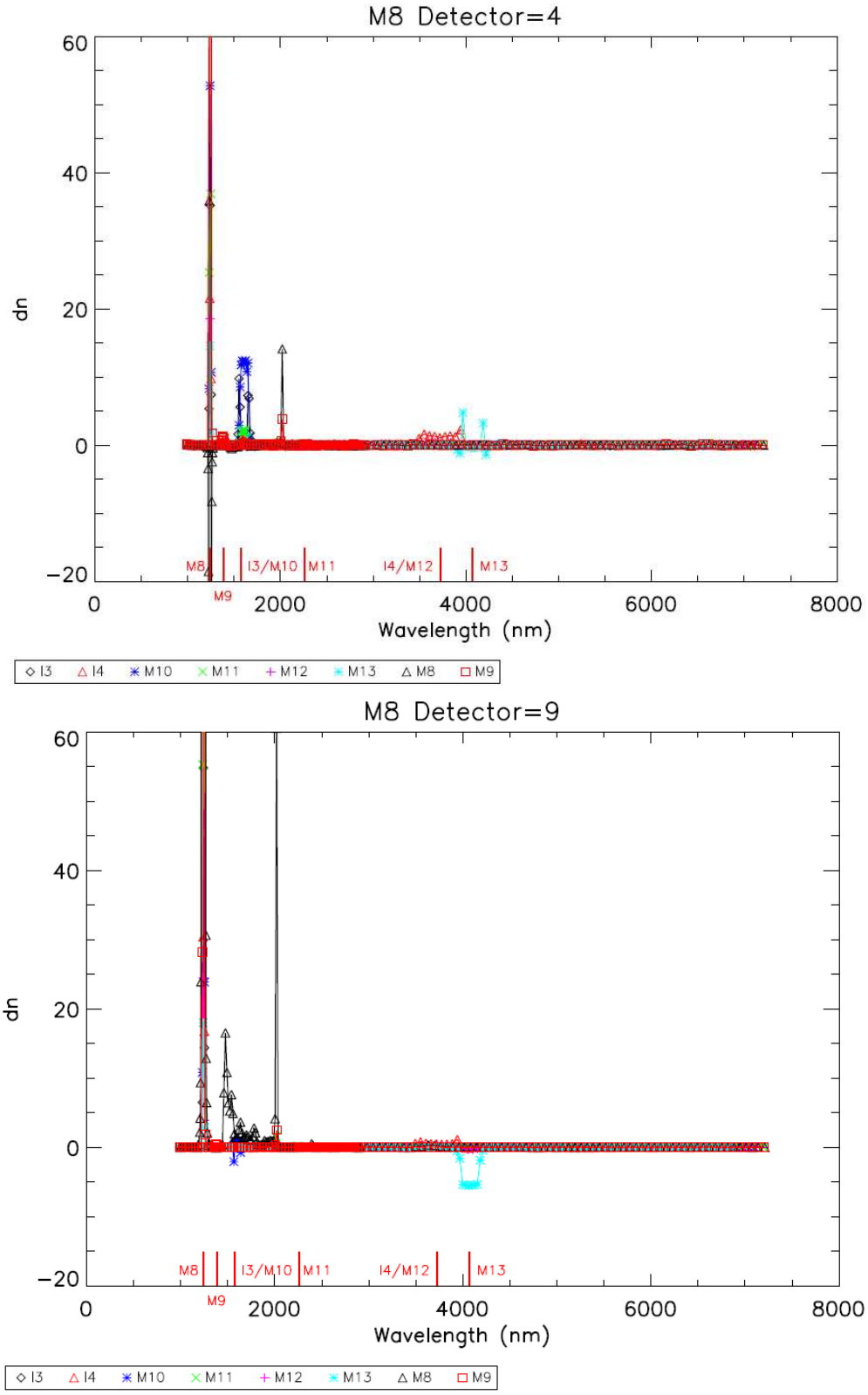

Figure 6: Response as a function of wavelength and slit position for the M9 detectors 4 and 7.

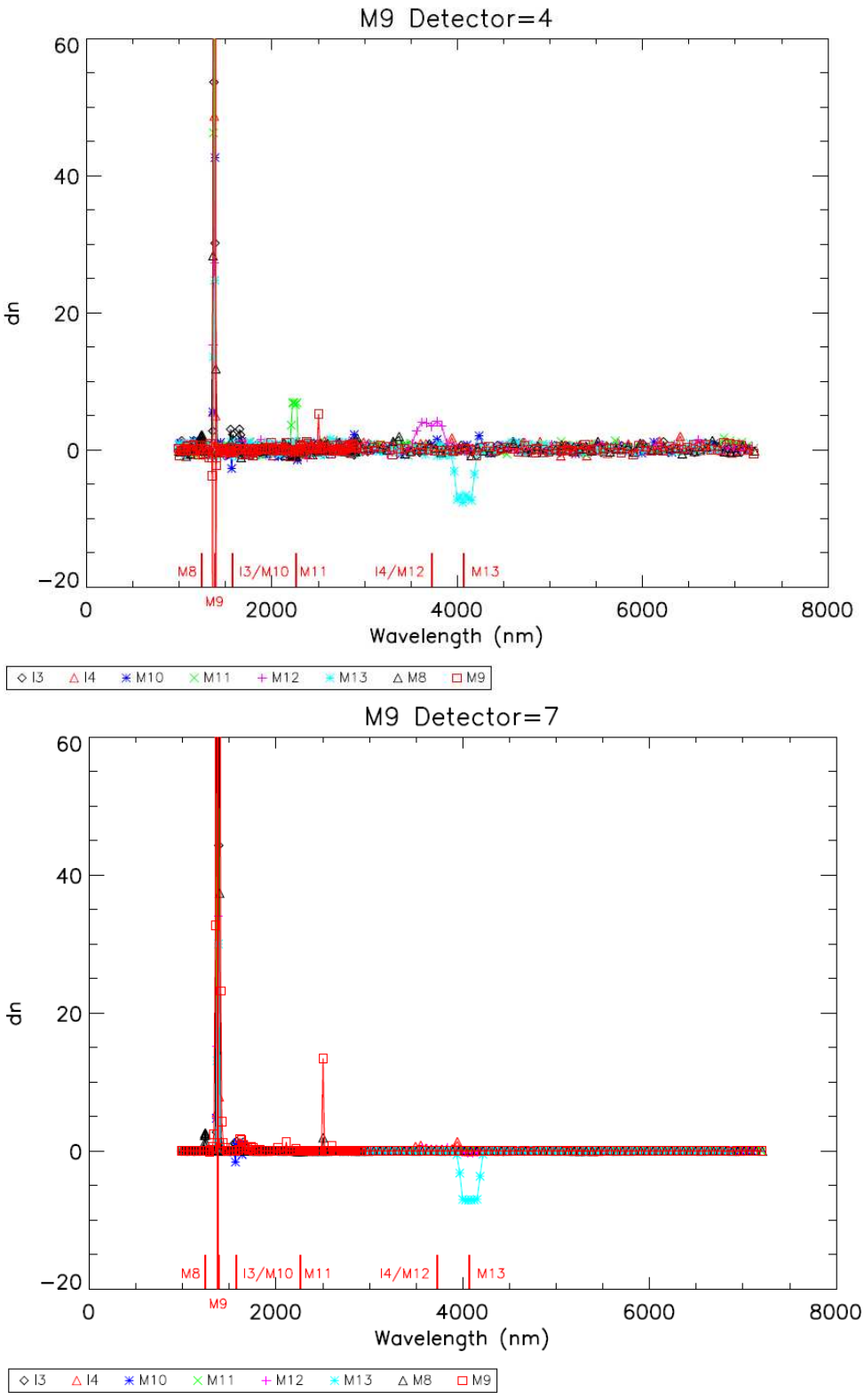

Figure 7: Response as a function of wavelength and slit position for the M10 detectors 4 and 9.

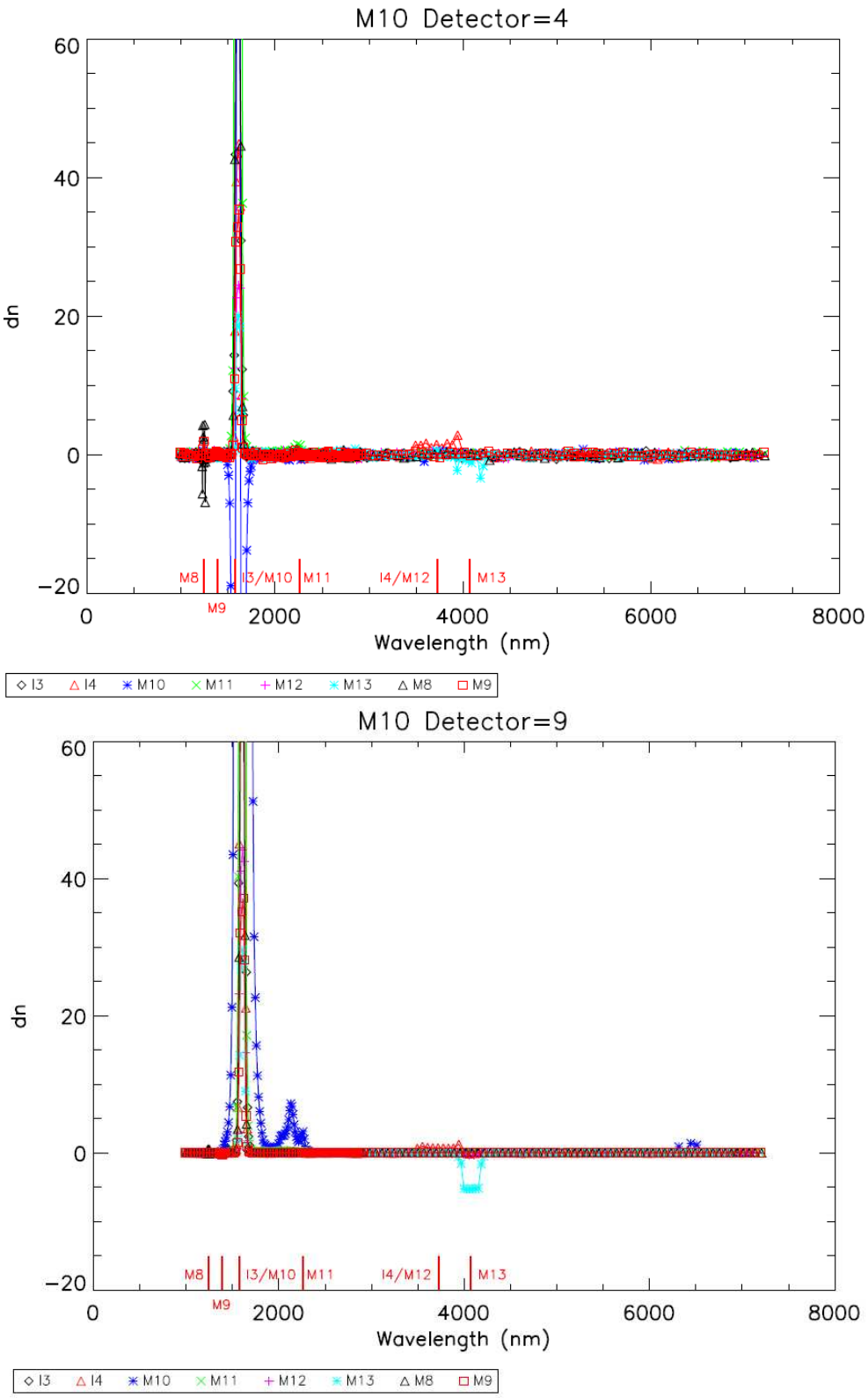

Figure 8: Response as a function of wavelength and slit position for the M11 detectors 9 and 12.

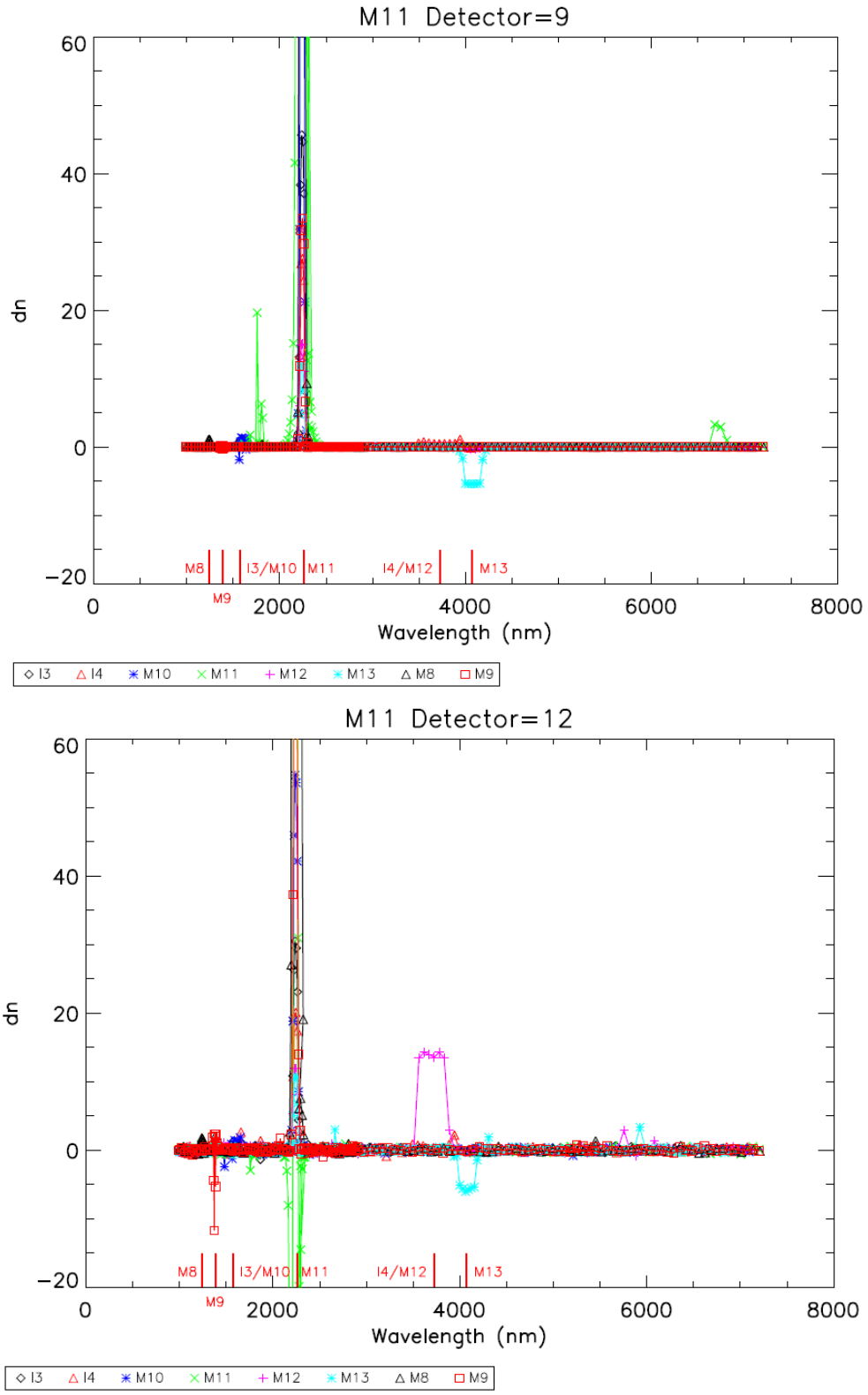

Figure 9: Response as a function of wavelength and slit position for the M12 detectors 9 and 12.

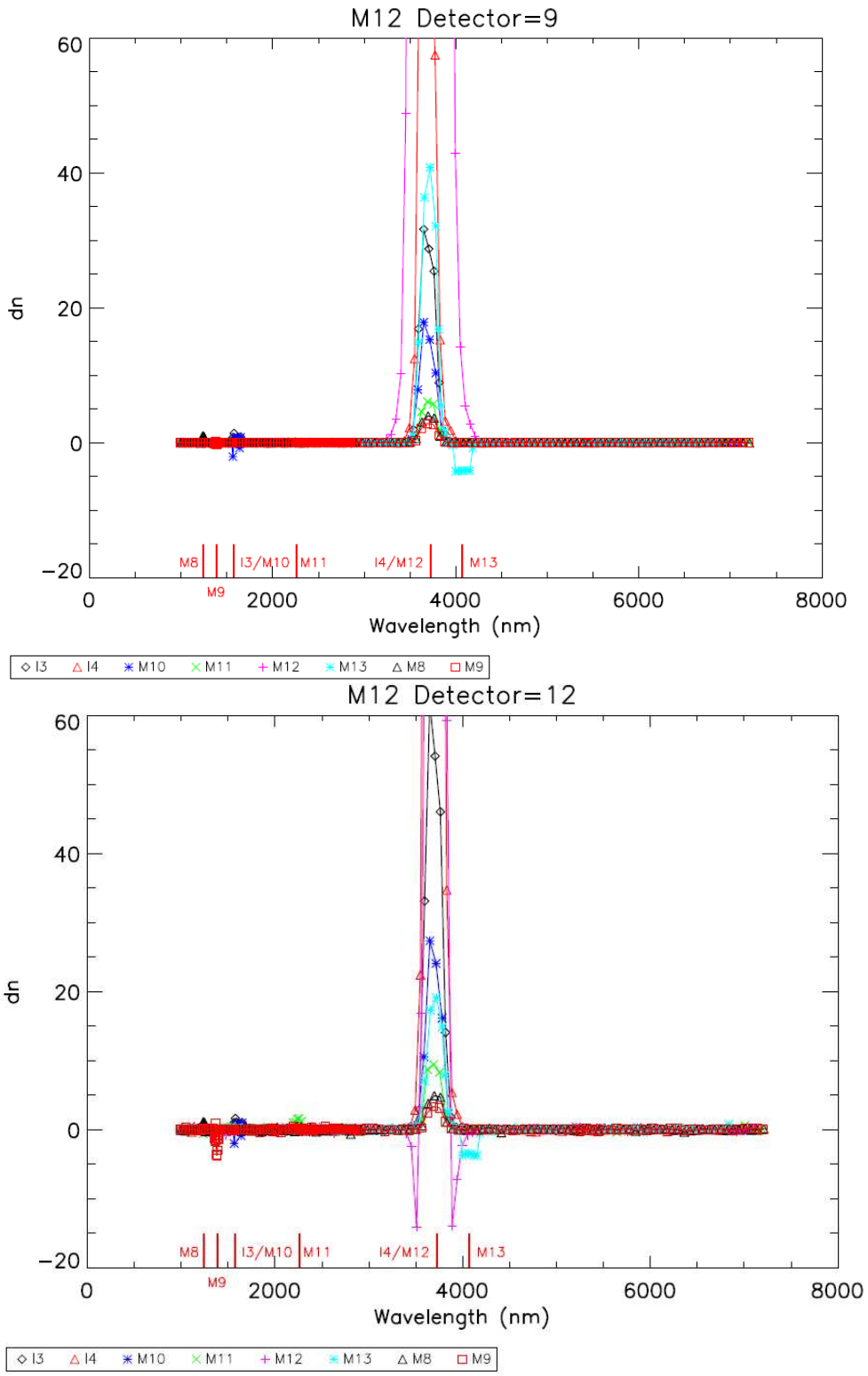

Figure 10: Response as a function of wavelength and slit position for the M13 detectors 4 and 9.

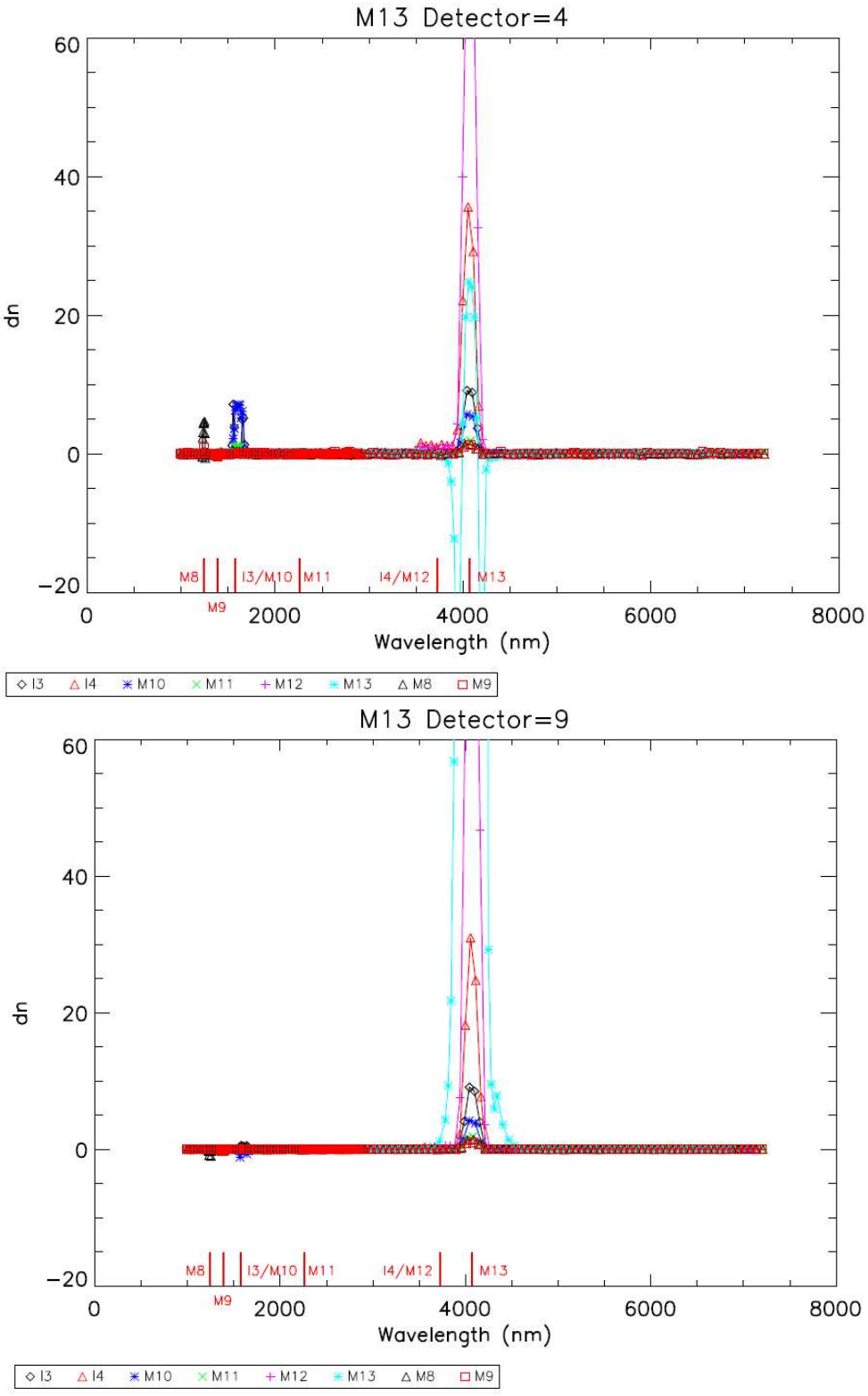

Figure 11: Percent crosstalk as a function of wavelength and slit position for the I3 SS1 detector 21.

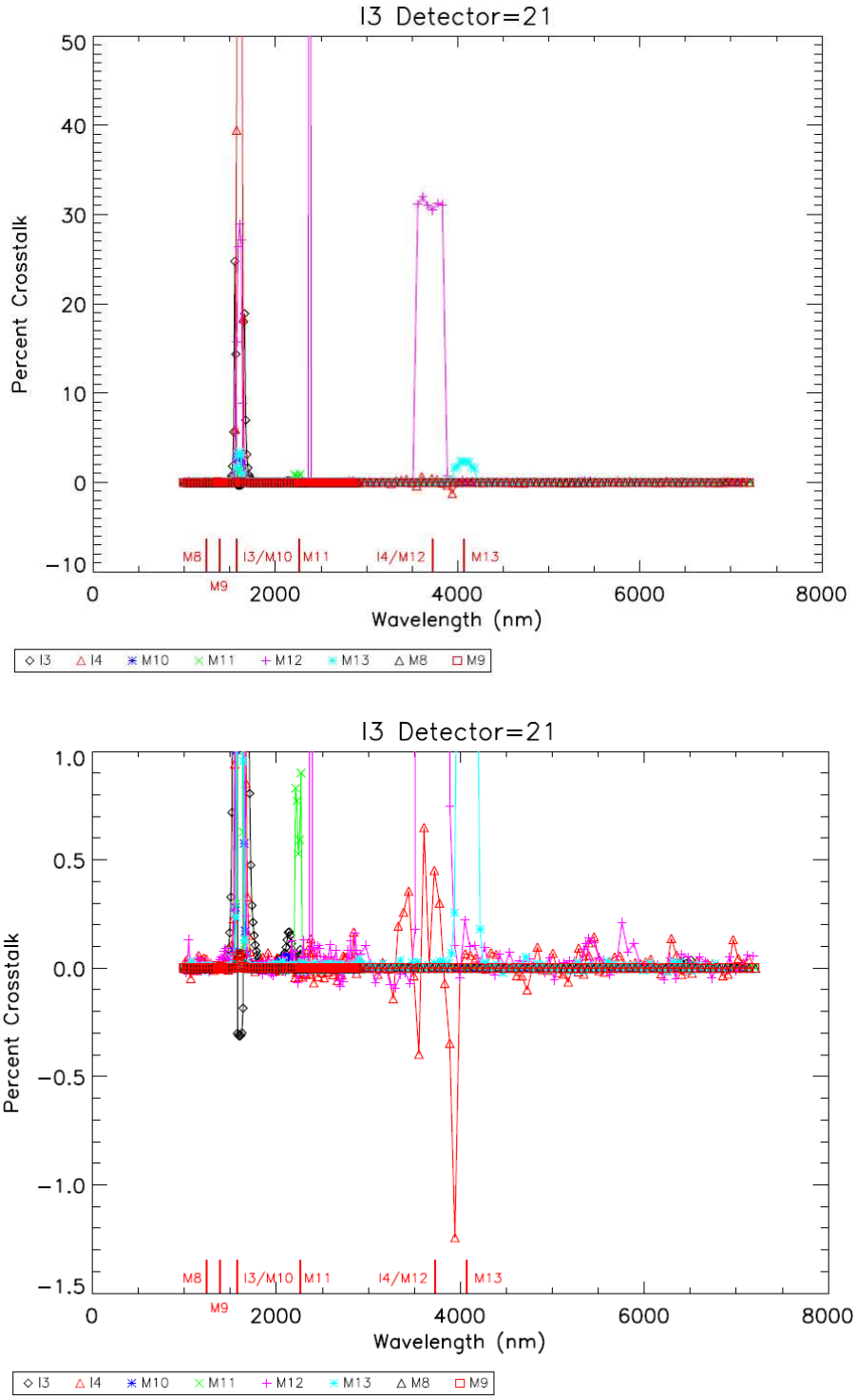

Figure 12: Percent crosstalk as a function of wavelength and slit position for the I4 SS1 detector 17.

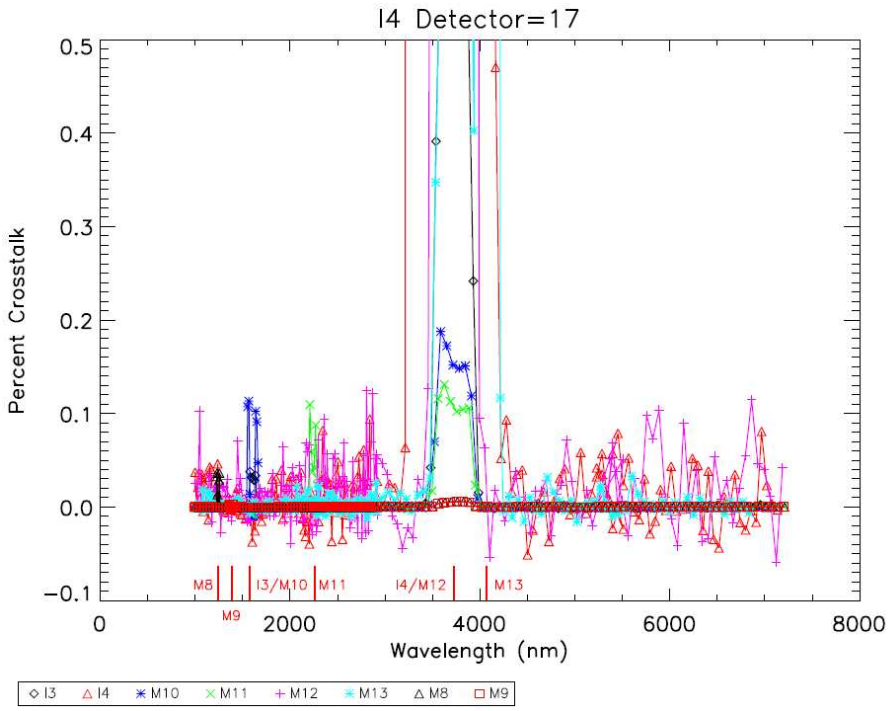

Figure 13: Percent crosstalk as a function of wavelength and slit position for the M8 detector 5.

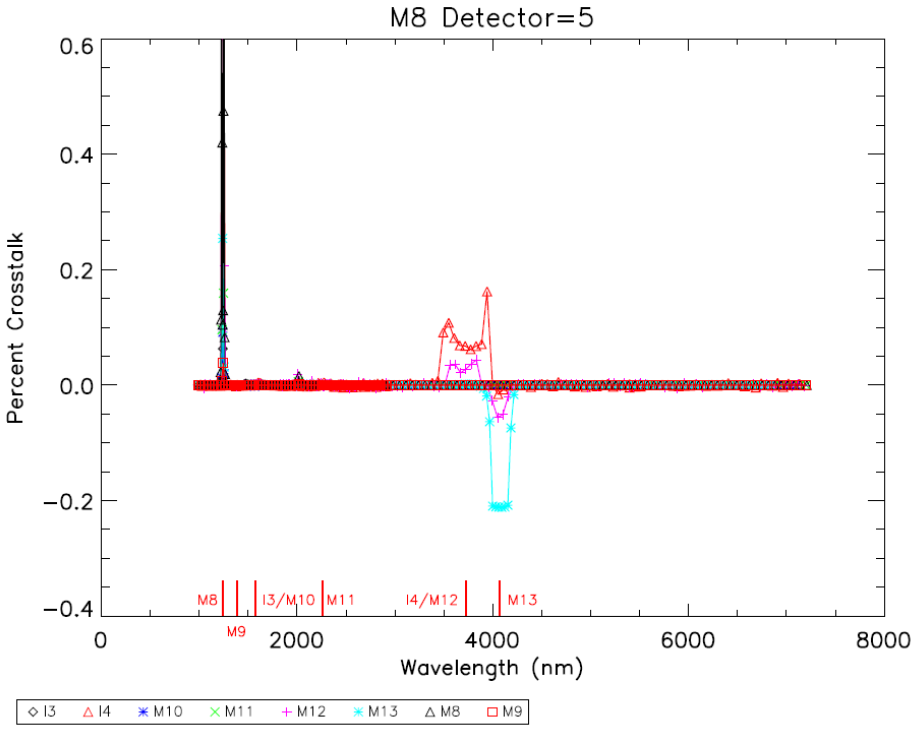

Figure 14: Percent crosstalk as a function of wavelength and slit position for the M9 detector 21.

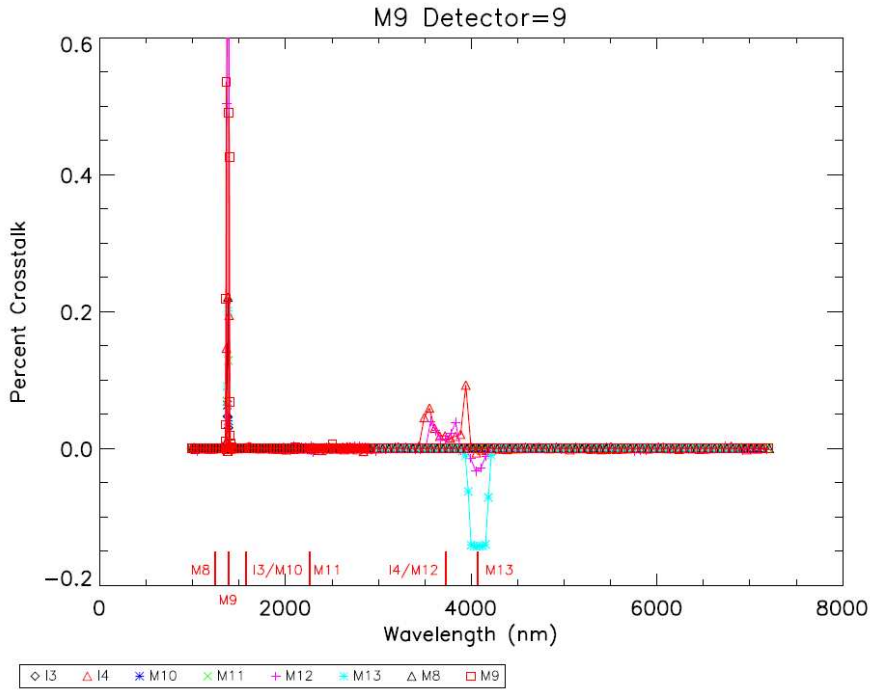

Figure 15: Percent crosstalk as a function of wavelength and slit position for the M10 detector 5.

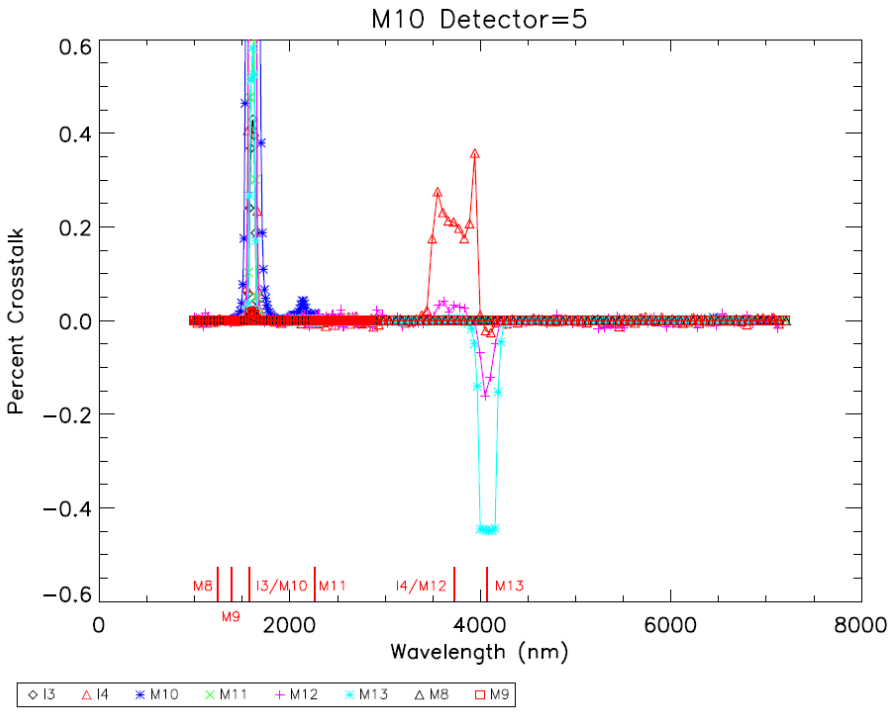

Figure 16: Percent crosstalk as a function of wavelength and slit position for the M11 detector 9.

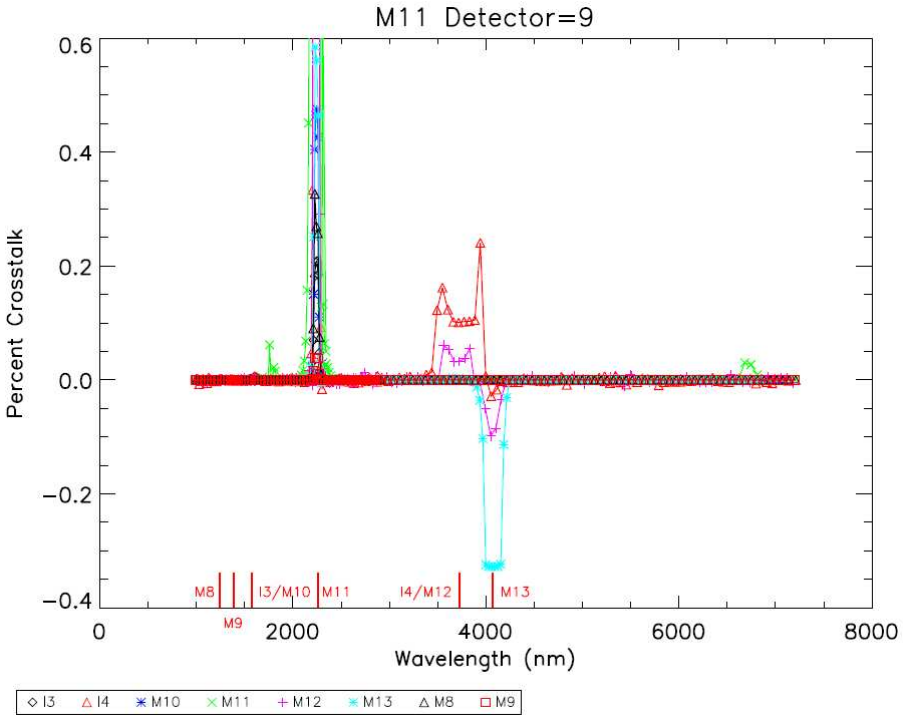

Figure 17: Percent crosstalk as a function of wavelength and slit position for the M12 detector 9.

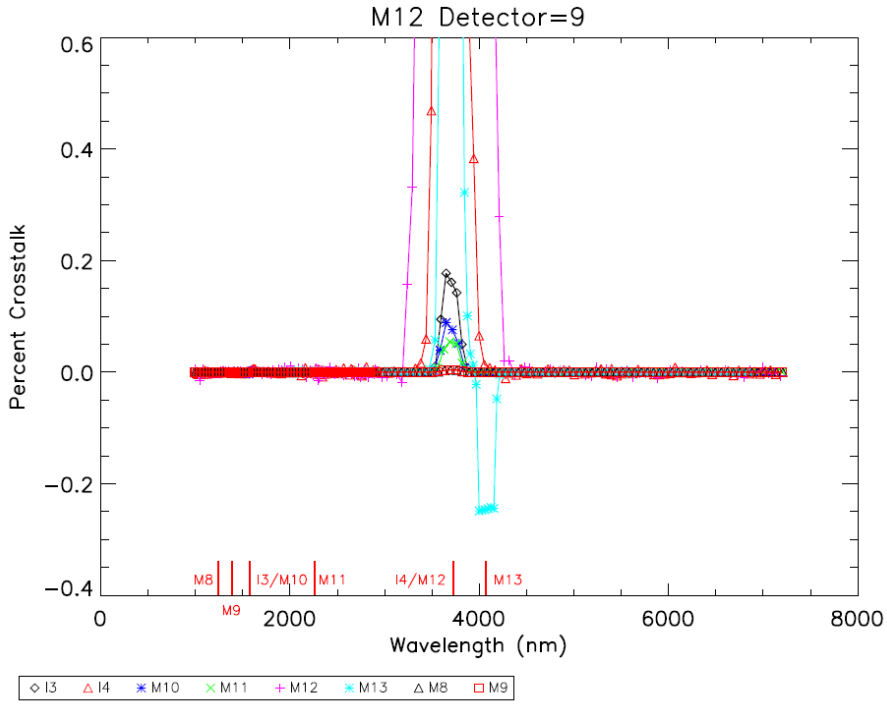

Figure 18: Percent crosstalk as a function of wavelength and slit position for the M13 detector 9.

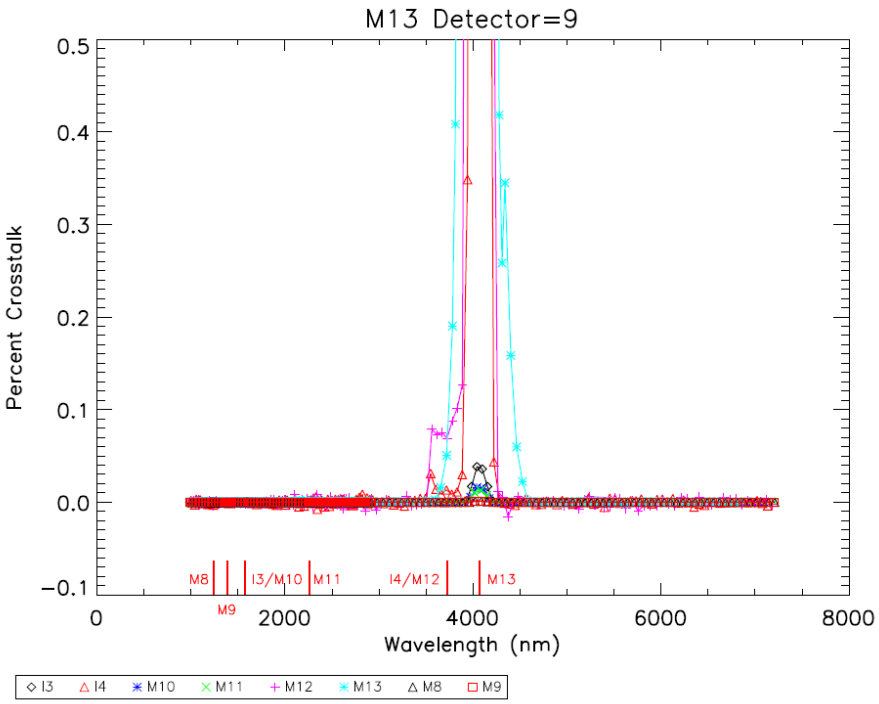

Figure 19: Response as a function of wavelength and slit position for the I5 SS1 detector 27.

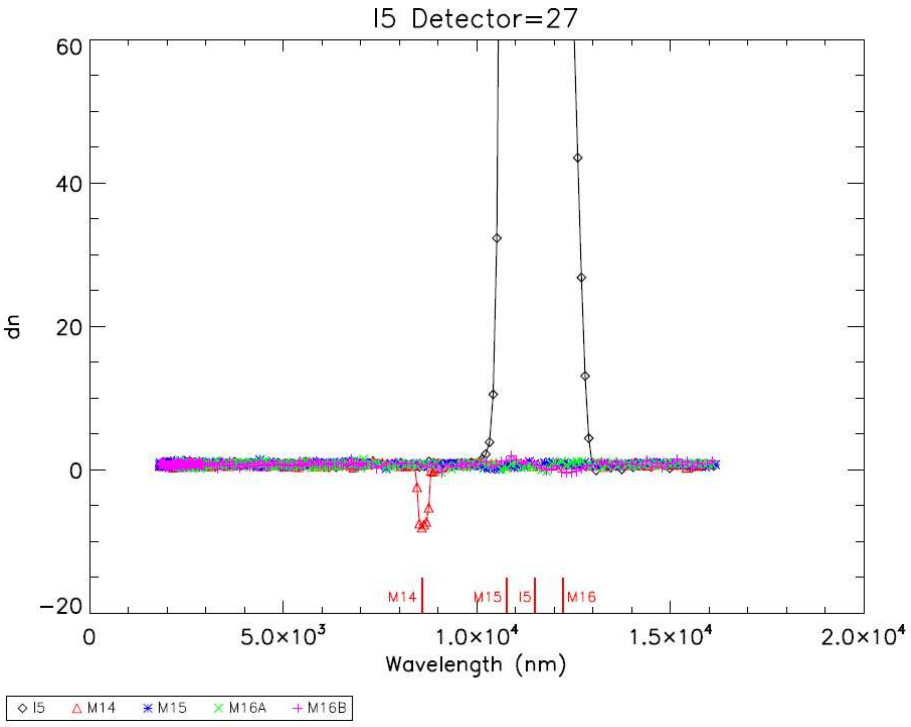

Figure 20: Response as a function of wavelength and slit position for the M14 detectors 9 and 10.

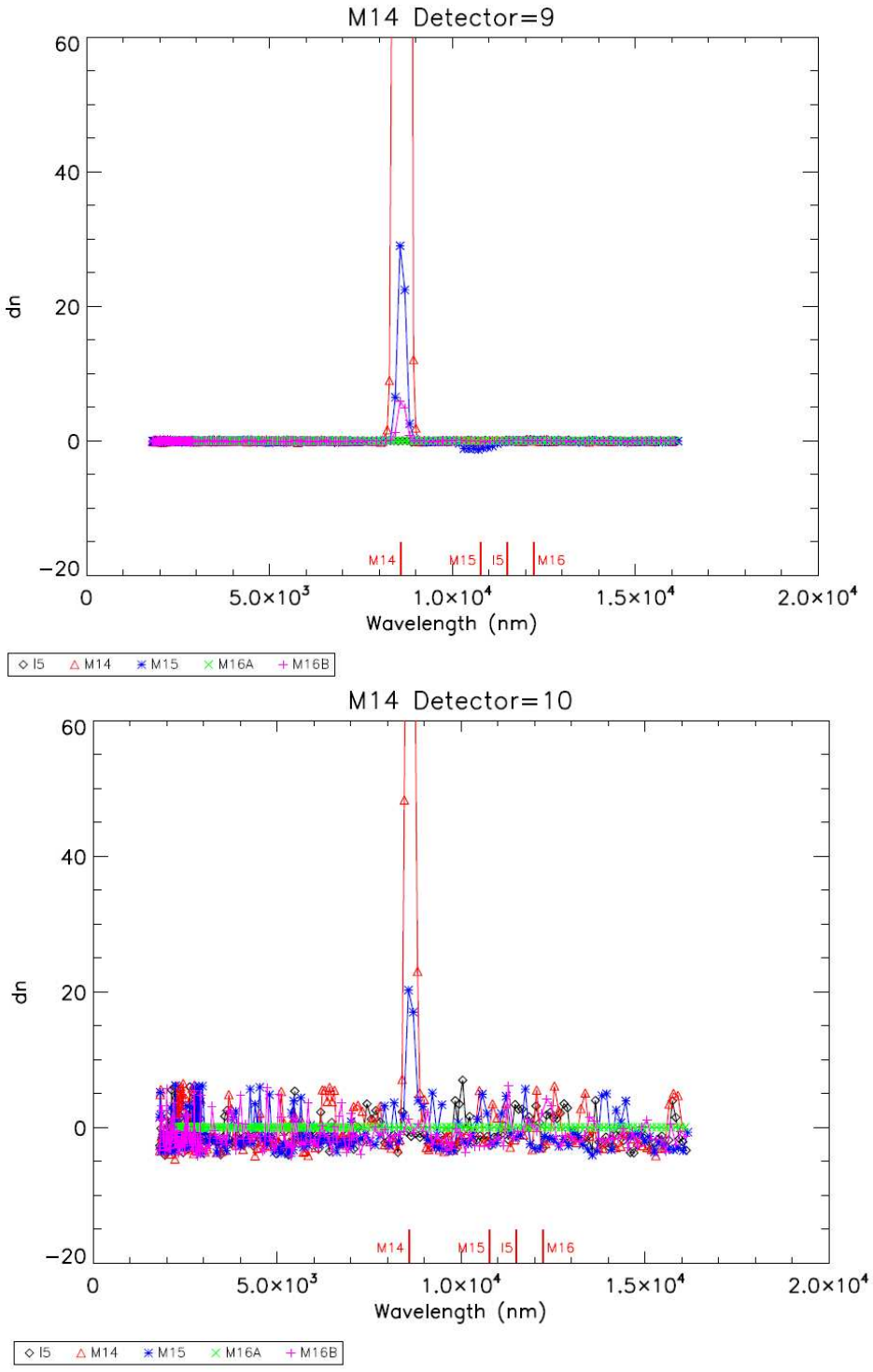

Figure 21: Response as a function of wavelength and slit position for the M15 detector 9.

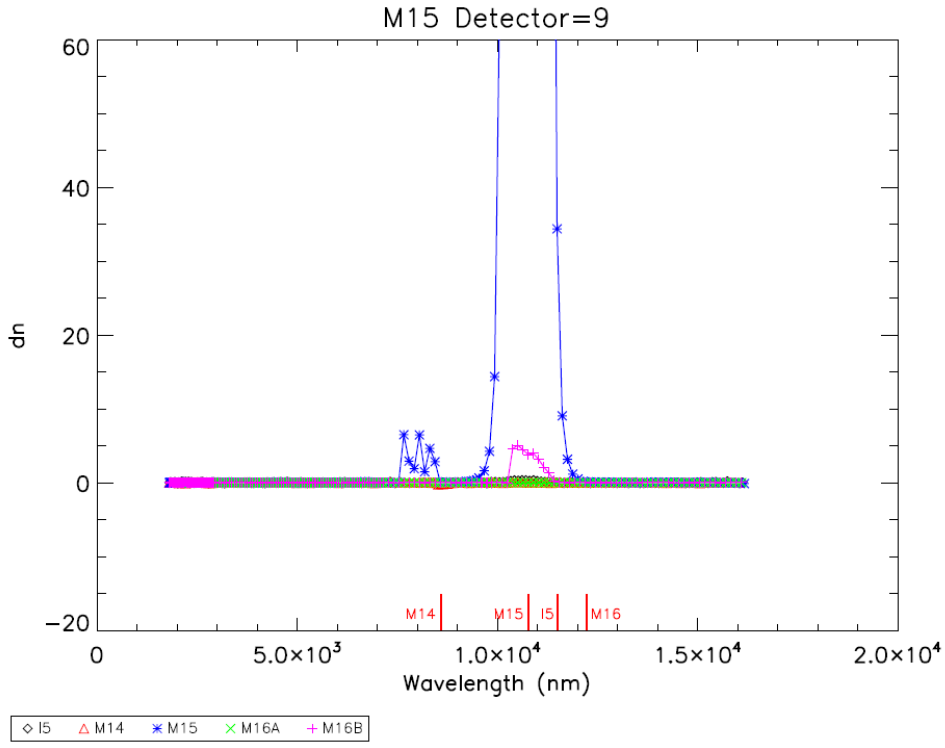

Figure 22: Response as a function of wavelength and slit position for the M16A detector 9.

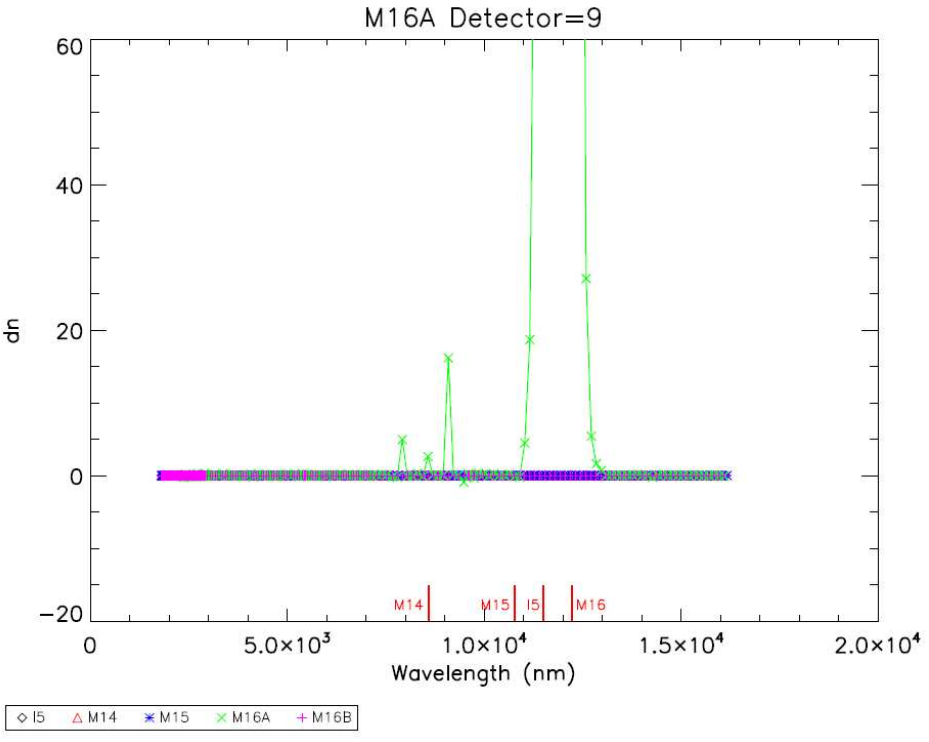

Figure 23: Response as a function of wavelength and slit position for the M16B detectors 9 and 16.